Synthesis and Design of a New Printed Filtering Antenna

Shyh-Jong Chung

Department of Communication Engineering, National Chiao-Tung University
1001 Tahsueh Rd., Hsinchu, 300, Taiwan

摘要— 本計劃提出新型印刷式濾波天線之合成與設計，利用共同設計 (co-design) 之方法，使濾波器與天線達到有效的整合與簡單製作之需求。本次研究使用印刷式倒L型天線 (inverted-L antenna) 與平行耦合之微帶線 (parallel coupled microstrip line) 來實現帶通濾波天線。首先建立串聯RLC形式之倒L型天線的等效電路，並與全波模擬的結果做比較，粹取其等效電路之元件參數的值。在此，倒L型天線不僅可作為一個輻射體，還可作為濾波器最後一階的共振器。詳細的設計步驟在本文亦被提出，可透過濾波器之規格來實現之。以操作頻率為2.45GHz且具0.1 dB 等漣波響應之三階柴比雪夫濾波器為例子來設計一濾波天線，並與傳統之設計方法(即濾波器與天線各別設計後再合成)做比較，所提出之架構有較好的設計準確性與濾波器邊緣選擇性，且不佔據太多的電路面積。所量測之結果與設計的做比較，包括折反損耗(return loss)、輻射增益對頻率(radiation gain versus frequency)之響應，具有良好的一致性。

關鍵字—柴比雪夫帶通濾波器，濾波天線，濾波器合成，倒L型天線，邊緣選擇性。

Abstract— Synthesis and design of a new printed filtering antenna is presented in this proposal. For the requirements of efficient integration and simple fabrication, the co-design approach for the integration of filter and antenna is introduced. The printed inverted-L antenna and the parallel coupled microstrip line sections are used for example to illustrate the synthesis of a bandpass filtering antenna. The equivalent circuit model for the inverted-L antenna, which is mainly a series RLC circuit, is first established. The values of the corresponding circuit components are then extracted by comparing with the full-wave simulation results. The inverted-L antenna here performs not only a radiator but also the last resonator of the bandpass filter. A design procedure is given, which clearly indicates the steps from the filter specifications to the implementation. As an example, a 2.45 GHz third-order Chebyshev bandpass filter with 0.1 dB equal- ripple response is tackled. Compared to the traditional filter and antenna designed separately, the proposed structure provides more design accuracy and good filter skirt selectivity, while without suffering more circuit area. The measured results, including the return loss and the radiation gain versus frequency, agree well with the designed ones.

Index Terms—Chebyshev bandpass filter, filtering antenna, filter synthesis, inverted-L antenna, skirt selectivity.

I. INTRODUCTION

IN many wireless communication systems, the RF filters are usually placed right after the antenna. Since the size reduction and low profile structure are a trend in the circuit design, it is desired to integrate the bandpass filter and antenna in a single module, so called *filtering antenna*, with filtering and radiating functions simultaneously. However, to date, there has been relatively little research conducted on an efficient integration between the filter and antenna with simple fabrication and good circuit behavior. In traditional design, the filter and the antenna are designed individually, with the common ports' characteristic impedance Z_0, and then connected directly. An example of this filter cascaded with antenna is shown in Fig. 1 (a), which presents a second-order bandpass filter in cascade with an

inverted-L antenna. The direct connection of the filter and antenna usually causes an impedance mismatch, which may deteriorate the filter's performance (especially near the band edges) and increase the insertion loss of the circuitry. To avoid this, extra matching network should be implemented in between these two components [1].

Several investigations have been focused on adding the radiating or filtering function into an antenna or filter [2-4]. In [2], metal posts were inserted into a horn antenna, which can generate the filtering function. And in [3], the way is to create coupled cavities into a leaky wave antenna so as to generate filtering performance on the antenna. Frequency selectivity surface using cascading substrate integrated waveguide cavity had been designed and directly installed at the aperture of horn antenna [4]. While these proposed circuits possess the characteristics of filtering and radiating, it should be noted that they were designed without using a systematic approach nor considering much on the filter's or antenna's specifications.

Various approaches for integrating the filter and antenna into a single microwave device have been discussed in [5]-[10]. For size reduction, a pre-designed bandpass filter with suitable configuration was directly inserted into the feed position of a patch antenna [5] and a horn antenna [6]. By using an extra impedance transformation structure in between the filter and the antenna, the bandpass filter can be integrated properly with the antenna over the required bandwidth [7]-[9]. However, the transition structure needs additional circuit area, and the designs did not have good filter characteristics over the frequency range. In [10], a mutual synthesis approach was proposed, which considered the conjugate impedance matching in between the filter and antenna. It seems that the matching was performed only at the center frequency, without considering the effect of the antenna's bandwidth and quality factor.

Recently, several filtering antennas designed following the synthesis process of the bandpass filter have been presented [11]-[14]. In these designs, the last resonator and the load impedance of the bandpass filter were substituted by an antenna that exhibited a series or parallel RLC equivalent circuit.

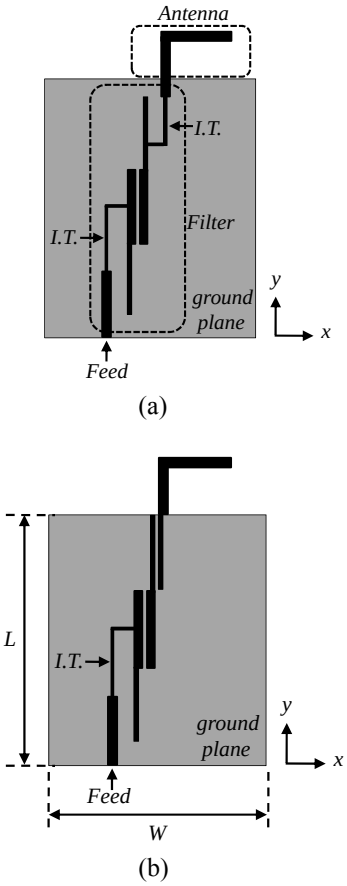

Fig. 1. Configurations of (a) the traditional filter cascaded with antenna and (b) the proposed filtering antenna. I.T. = Impedance Transformer.

Although they have been done based on the co-design approach, Most of them did not show good filter performance, especially the band-edge selectivity and stopband suppression. This is due to the lack of the extraction of the antenna's equivalent circuit over a suitable bandwidth. Only that at the center frequency was extracted and used in the filter synthesis. Moreover, the antenna gain versus frequency, which is an important characteristic of the filtering antenna, was not examined in these studies. Although in [14], the frequency response of a factor named *ideal matching loss* (= $1-|S_{11}|^2$) was considered, it did not take into account the circuit and antenna losses and thus missed the power transmission characteristic of the filtering antenna.

In this proposal, a new co-design method is proposed to achieve a filtering antenna with printed structure as shown in Fig. 1 (b). The printed inverted-L antenna is used with its equivalent circuit completely extracted over a desired bandwidth for the synthesis of the filtering antenna. Also, to

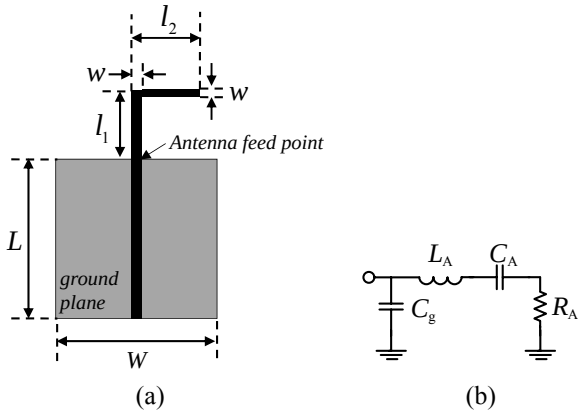

Fig. 2. (a) Geometry of the inverted-L antenna and (b) the corresponding equivalent circuit model.

increase the fabrication tolerance, a quarter-wave admittance inverter with characteristic impedance other than Z_0 is introduced in the filter synthesis.

II. Equivalent Circuit Model of the Inverted-L Antenna

Since the antenna is to be designed in the filter as the last resonator, the first step to synthesize the filtering antenna is to establish the antenna's equivalent circuit model and extract the circuit components. Figs. 2 (a) and (b) show the dimensions of the inverted-L antenna and the corresponding equivalent circuit at the antenna feed point looking toward the antenna. Since the inverted-L antenna is a variety of a monopole antenna, the antenna exhibits a series RLC resonance near the first resonant frequency [15]. Here, L_A and C_A express the resonant inductance and capacitance of the antenna, respectively, and R_A corresponds to the antenna radiation resistance. It is noted that an extra shunt capacitance C_g is incorporated in the equivalent circuit here so that, as will be seen below, the whole circuit would have the same impedance behavior as the antenna itself in a wider frequency range. This parasitic capacitance comes from the accumulation of charges around the antenna feed point due to the truncation of the ground plane.

The antenna resistance R_A in the equivalent circuit can serve as the load impedance of the bandpass filter to be synthesized, and the series L_A-C_A circuit can be the filter's last resonator so that

$$f_0 = \frac{1}{2\pi\sqrt{L_A C_A}} \tag{1}$$

where f_0 is the center frequency of the bandpass filter. Note that owing to the existence of the parasitic capacitance, the resonant frequency f_A of the antenna is higher than f_0. This means that, in order to attain (1), the antenna should be designed at a frequency higher than the bandpass filter frequency. In this work, f_0 is set as 2.45 GHz, and the required antenna frequency f_A is calculated to be 2.53 GHz.

The inverted-L antenna is printed on a 0.508 mm Rogers 4003 substrate with a dielectric constant of 3.38 and loss tangent of 0.0027. The ground plane of the antenna, which is also the ground plane of the circuitry, has a fixed size of $L \times W = 60$ mm $\times$ 60 mm. The antenna is fed through a 50 Ω microstrip line of width 1.17 mm. In this design, the full-wave simulation solver HFSS [16] is used. For each given inverted-L antenna structure, the equivalent circuit components are extracted by first letting the resonant frequency of the circuit equal the simulated resonant frequency of the antenna. And then, we optimize the values of the circuit components so that the reflection coefficient (S_{11}), as a function of frequency, of the equivalent circuit coincides with that simulated from the antenna in a frequency range as wide as possible. The difference ΔS_{11} of the reflection coefficient between these two curves is set not beyond 3% in a 20% frequency bandwidth centered at the antenna resonant frequency. In the mean time, the inductance L_A and capacitance C_A should follow the relationship of (1) for a given bandpass filter with the frequency f_0 (= 2.45 GHz). Accordingly, the equivalent circuit components for different dimensions of the inverted-L antenna are obtained.

Fig. 3 depicts the variations of the extracted component values as the vertical strip length l_1 is changed from 5 mm to 13 mm. The strip width w is fixed as 1.17 mm, the same as the feed line width, and the horizontal strip length l_2 is determined according to l_1 so that the antenna has a resonant frequency at f_A = 2.53 GHz. It is observed from the figure that, the inductance L_A and resistance R_A increase, while the capacitance C_A decreases, as l_1 becomes larger. Here, the curves of L_A and C_A have opposite trends due to (1). The increases of L_A and R_A are reasonable, since the quarter-wavelength inverted-L antenna has the strongest current distributed on the vertical strip l_1 so that a larger l_1 would contribute to more radiation resistance and

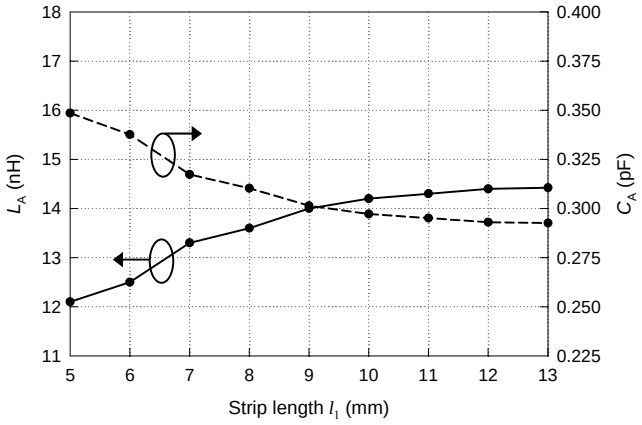

(a)

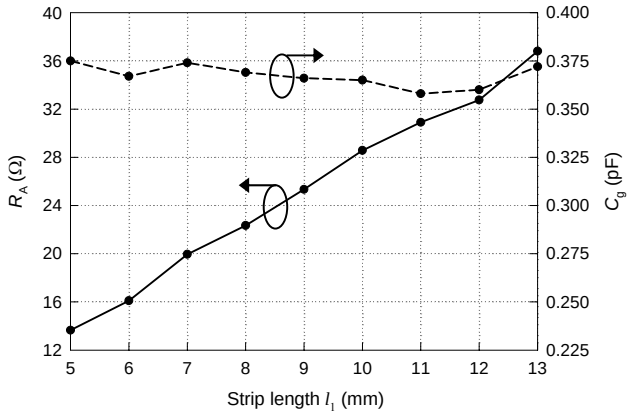

(b)

Fig. 3. Extracted component values of the inverted-L antenna's equivalent circuit, as functions of the strip length l_1. (a) L_A and C_A. (b) R_A and C_g. w = 1.17 mm.

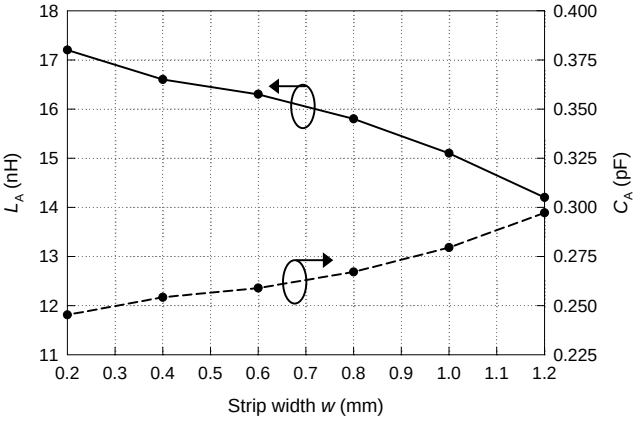

(a)

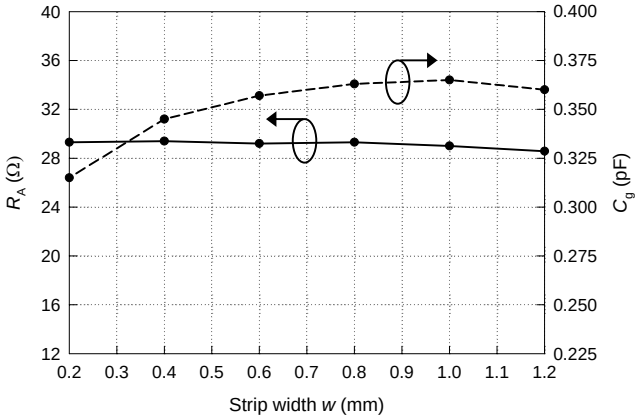

(b)

Fig. 4. Extracted component values of the inverted-L antenna's equivalent circuit, as functions of the strip width w. (a) L_A and C_A. (b) R_A and C_g. l_1 = 10 mm.

larger inductance. Besides, the parasitic capacitance C_g is roughly independent of l_1, which has a value near 0.37 pF. Notice that this capacitance is about equal to, if not larger than, C_A, and thus cannot be neglected in the modeling of the antenna.

Fig. 4 illustrates the changes of the equivalent circuit components for varied strip width w from 0.2 mm to 1.2 mm. The strip lengths are fixed with l_1 = 10 mm. It is obvious that the inductance L_A increases, and the capacitance C_A decreases accordingly, as w decreases. In addition, the radiation resistance R_A is around 29 Ω for all strip widths considered since its value is mainly determined by l_1. Here we can find that the parasitic capacitance C_g is varied slightly between 0.3 pF and 0.4 pF.

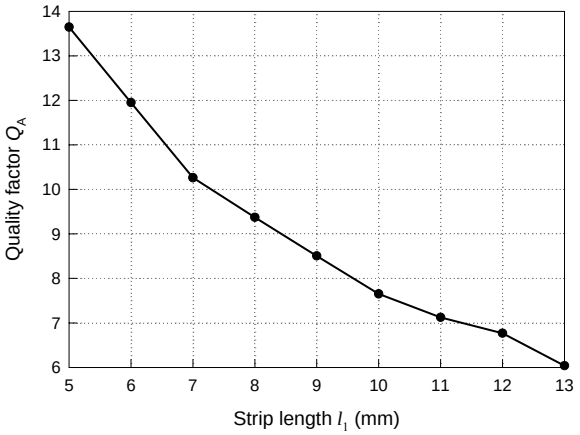

Fig. 5. The antenna quality factor Q_A as a function of the strip length l_1. w = 1.17 mm, f = 2.45 GHz.

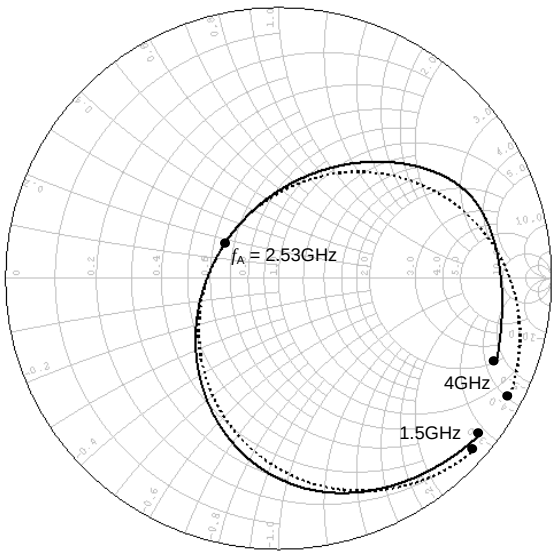

Fig. 6. Input impedances of the inverted-L antenna with l_1 = 10 mm, w = 1.17 mm, and l_2 = 17.25 mm. (solid line: simulated results; dotted line: results from equivalent circuit.)

Since the antenna is to be used as the last resonator of the bandpass filter, the corresponding quality factor is an important parameter in the synthesis of the filter. Here, the quality factor of the antenna, Q_A, is defined as

$$Q_A = \frac{2\pi f_0 L_A}{R_A} \tag{2}$$

which is that of the series RLC circuit in the antenna's equivalent circuit, without including the effect of the parasitic capacitance C_g. It should be noticed that the Q_A is not the whole quality factor of the inverted-L antenna. Fig. 5 shows the variation of the quality factor as a function of the strip length l_1, which illustrates the decreasing of the quality factor as the strip length increases. This trend can be expected if one observes the variations of L_A and R_A in Fig. 3. It is seen that, although L_A and R_A both become larger with increased strip length, the radiation resistance increases much fast then the inductance. The quality factor decreases from 13.7 to 6 when l_1 increases from 5 mm to 13 mm. Although not shown here, the quality factor has little change as the strip width w varied. This is because that, from Fig. 4, both L_A and R_A are slow varying functions of w. The quality factor changes from 7.5 to 9 when the strip width decreases from 1.2 mm to 0.2 mm.

Fig. 6 shows the comparison of the impedance behaviors on the Smith chart from the full-wave simulation and the equivalent circuit calculation. The dimensions of inverted-L antenna, which is to be used later in the synthesis of the filtering antenna, are l_1 = 10 mm, w = 1.17 mm, and l_2 = 17.25 mm. And the corresponding circuit components extracted above are L_A = 14.2 nH, C_A = 0.30 pF, R_A = 28.6 Ω, and C_g = 0.37 pF. The curve of S_{11} for the equivalent circuit agrees well with the simulation one from 1.5 GHz to 4 GHz. Especially, they have the same value at the antenna resonant frequency (f_A = 2.53 GHz), and the difference ΔS_{11} is 0.16 dB (error of $\Delta S_{11} \approx 3\%$) at f = 2.28 GHz and 0.148 dB (error of $\Delta S_{11} \approx 3\%$) at f = 2.81 GHz. Note that the curves do not pass through the original point at the resonant frequency due to the lower antenna radiation resistance.

III. Synthesis of the Filtering Antenna

Fig. 7 (a) shows the proposed filtering antenna, which contains three coupled line sections and an inverted-L antenna. Note that the antenna is connected directly to the third coupled line. The filter to be synthesized is a third-order Chebyshev bandpass filter. The first two filter resonators are provided by the coupled line sections and the last one by the inverted-L antenna. In order to match to the low antenna radiation resistance and increase the flexibility of design, here the last coupled line has different design as the conventional ones [17]. Consider a coupled line section with even- and odd-mode characteristic impedances Z'_{0e3} and Z'_{0o3}, respectively, as shown in Fig. 8 (a). This coupled line is to be equivalent to the circuit shown in Fig. 8 (b) near the center frequency f_0. Note that the right transmission line section has a characteristic impedance Z_a, which is different from the system impedance Z_0 (= 50 Ω) and can be selected arbitrarily. The ABCD matrices of the coupled line section and the equivalent circuit are derived as

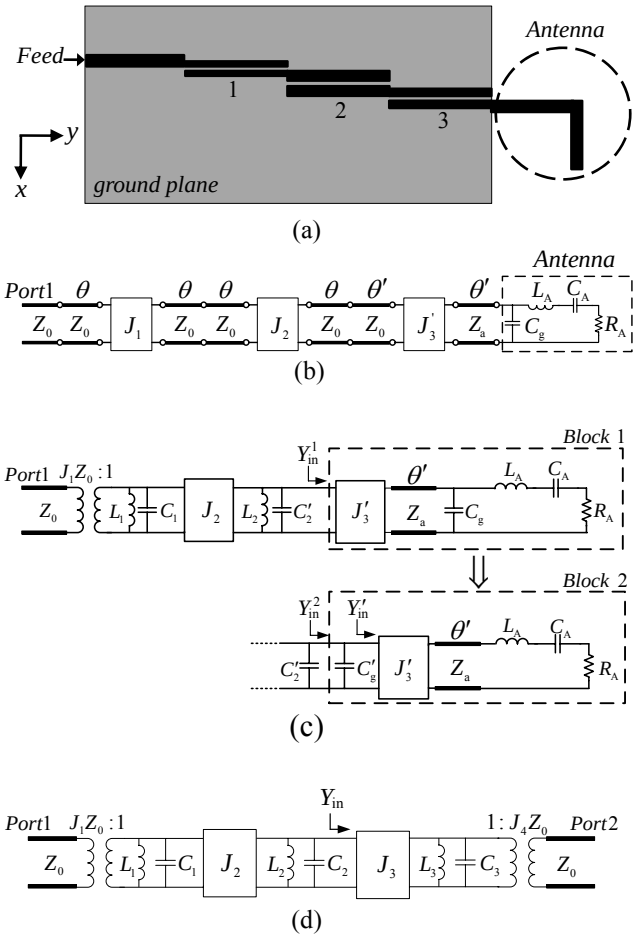

Fig. 7. (a) The structure of the proposed third-order filtering antenna. (b) Equivalent circuit of the proposed filtering antenna. (c) Modified circuit of the proposed filtering antenna. (d) A typical third-order bandpass filter circuit using shunt resonators with admittance inverters.

$$\begin{bmatrix} A & B \\ C & D \end{bmatrix}_{\substack{coupled \\ line}} = \begin{bmatrix} \dfrac{Z'_{0e3}+Z'_{0o3}}{Z'_{0e3}-Z'_{0o3}}\cos\theta' & \dfrac{j}{2}\left\{(Z'_{0e3}-Z'_{0o3})\sin\theta' - \dfrac{4Z'_{0e3}Z'_{0o3}\cos^2\theta'}{(Z'_{0e3}-Z'_{0o3})\sin\theta'}\right\} \\ j\dfrac{2}{Z'_{0e3}-Z'_{0o3}}\sin\theta' & \dfrac{Z'_{0e3}+Z'_{0o3}}{Z'_{0e3}-Z'_{0o3}}\cos\theta' \end{bmatrix} \tag{3}$$

$$\begin{bmatrix} A & B \\ C & D \end{bmatrix}_{\substack{equival \\ circuit}} = \begin{bmatrix} \left(J_3'Z_0 + \dfrac{1}{J_3'Z_a}\right)\sin\theta'\cos\theta' & j\left(J_3'Z_0Z_a\sin^2\theta' - \dfrac{\cos^2\theta'}{J_3'}\right) \\ j\left(\dfrac{1}{J_3'Z_0Z_a}\sin^2\theta' - J_3'\cos^2\theta'\right) & \left(J_3'Z_a + \dfrac{1}{J_3'Z_0}\right)\sin\theta'\cos\theta' \end{bmatrix} \tag{4}$$

To have the same circuit performances near the center frequency, these two ABCD matrices should be equal at $\theta' = \pi/2$, resulting into

$$Z'_{0e3} = Z_a\left[\frac{Z_0}{Z_a} + J_3'Z_0 + \left(J_3'Z_0\right)^2\right] \tag{5a}$$

$$Z'_{0o3} = Z_a\left[\frac{Z_0}{Z_a} - J_3'Z_0 + \left(J_3'Z_0\right)^2\right] \tag{5b}$$

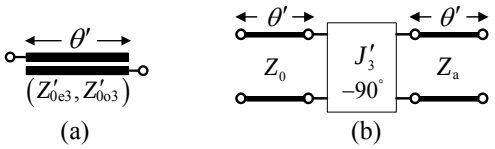

Fig. 8. (a) Geometry of the third coupled line section and (b) the corresponding equivalent circuit.

Therefore, once $J_3'Z_0$ is known, the impedances and thus the dimensions of the third coupled line section can be obtained.

By using the equivalent circuits of the antenna and the coupled line sections, the filtering antenna structure shown in Fig. 7 (a) can be expressed by the equivalent circuit shown in Fig. 7 (b). The two transmission line sections in between the admittance inverters have lengths equal to a half wavelength near the center frequency, i.e., $2\theta \approx \theta+\theta' \approx \pi$, and thus can be replaced by two parallel LC resonators as shown in the upper sub-figure of Fig. 7 (c). To transfer this circuit to a typical bandpass filter topology, the antenna's parasitic capacitance C_g should be moved to the left-hand side of the admittance inverter J_3' as illustrated in Block 2 of Fig. 7 (c). The resultant capacitance C_g' can be derived by equalizing the input admittances of Blocks 1 and 2 in the figure. The input admittance Y_{in}^1 of Block 1 is derived as

$$Y_{in}^1 = \frac{J_3'^2 Z_a\left[1/Z_a + jY_p\tan\theta'\right]}{Y_p + j\,1/Z_a\tan\theta'} \tag{6}$$

with

$$Y_p = j2\pi fC_g + \frac{1}{j\sqrt{\dfrac{L_A}{C_A}}\left(\dfrac{f}{f_0}-\dfrac{f_0}{f}\right) + R_A}$$

For frequencies near f_0, $\theta' \approx \pi/2$, and Y_{in}^1 can be approximated as

$$Y_{in}^1 \approx J_3'^2 Z_a^2\left(j2\pi fC_g + \frac{1}{j\sqrt{\dfrac{L_A}{C_A}}\left(\dfrac{f}{f_0}-\dfrac{f_0}{f}\right) + R_A}\right) \tag{7}$$

Also, the input admittance Y_{in}^2 of Block 2 at frequency near f_0 can be obtained as

$$Y_{in}^2 = j2\pi fC_g' + Y_{in}' \tag{8}$$

with

$$Y'_{\text{in}} \approx \frac{J_3'^2 Z_a^2}{j\sqrt{\frac{L_A}{C_A}}\left(\frac{f}{f_0}-\frac{f_0}{f}\right)+R_A} \tag{9}$$

By equalizing (7) and (8), one obtains

$$C'_g = (J'_3 Z_a)^2 C_g \tag{10}$$

Actually, the capacitance C'_g is much smaller than C'_2 (as will be seen in the next section), therefore, the total capacitance C_2 (= $C'_2 + C'_g$) of the second resonator is approximately equal to C'_2.

Finally, the equivalent circuit of Fig. 7 (c) can be transferred to the conventional third-order bandpass filter circuit, as shown in Fig. 7(d), by letting the admittance Y'_{in} equal Y_{in}, where

$$Y_{\text{in}} = \frac{J_3^2}{j\sqrt{\frac{C_3}{L_3}}\left(\frac{f}{f_0}-\frac{f_0}{f}\right)+Z_0 J_4^2} \tag{11}$$

From which, one obtains

$$Q_A = \frac{2\pi f_0 L_A}{R_A} = \frac{\pi}{2(Z_0 J_4)^2} \tag{12}$$

and

$$J'_3 Z_0 = \frac{J_3 Z_0}{Z_a}\left(\frac{2Q_A R_A Z_0}{\pi}\right)^{1/2} \tag{13}$$

The design procedures of the proposed filtering antenna can now be summarized as follows:

1) Specify the requirements of the bandpass filter to be synthesized, including the center frequency f_0, the fractional bandwidth Δ, and the type of the filter (e.g., bandpass filter with equal ripple), from which the admittance inverters J_nZ_0 (n = 1 ~ 4) and the parallel resonators L_n, C_n (n = 1 ~3) in Fig. 7 (d) can be determined [17].
2) Choose an antenna structure with suitable equivalent circuit that can substitute for the last resonator and load impedance of the bandpass filter. (Here in this study, the inverted-L antenna is used.) And then get a database associated with the equivalent circuit components for different antenna dimensions like those in Section II.
3) Calculate the antenna quality factor Q_A from (12) and then, after choosing a suitable strip width (e.g., the same width as the feed line), obtain the required strip length l_1 of the inverted-L antenna by using Fig. 5. To this end, all the component values of the antenna's equivalent circuit, and thus f_A, can be gotten from Fig. 3. The length l_2 of the horizontal antenna strip can thus be determined by letting the antenna resonate at f_A. The corresponding radiation resistance R_A can be read from Fig. 3(b). At this step, the dimensions of the inverted-L antenna are acquired.
4) Choose a suitable characteristic impedance Z_a (to be discussed in the next section) and then calculate the inverter constant J'_3Z_0 by using (13). Following, the even- and odd-mode characteristic impedances Z'_{0e3} and Z'_{0o3} of the third coupled line section for the proposed filtering antenna can be attained via (5).
5) By using the inverter constants J_nZ_0 (n = 1, 2) found in the first step, calculates the even- and odd-mode characteristic impedances Z_{0en} and Z_{0on} (n = 1, 2) of the first and second coupled line sections by the following formulae [17]:

$$Z_{0en} = Z_0\left[1 + J_nZ_0 + (J_nZ_0)^2\right]_{n=1,2} \tag{14a}$$

$$Z_{0on} = Z_0\left[1 - J_nZ_0 + (J_nZ_0)^2\right]_{n=1,2} \tag{14b}$$

6) Determine the dimensions of the three coupled line sections in the proposed filtering antenna by using the obtained even- and odd-mode characteristic impedances.

IV. Design Examples and Experimental Verification

In this section, an example of the proposed filtering antenna is to be presented. The filtering antenna is to be fabricated on a 0.508mm Rogers 4003 substrate with a dielectric constant of 3.38 and loss tangent of 0.0027. The ground plane size $L \times W$ = 60 mm × 60 mm. Following the above design procedures, a third-order Chebyshev bandpass filter with a 0.1 dB equal- ripple response is firstly chosen. The bandpass filter has a center frequency f_0 = 2.45 GHz, a fractional bandwidth Δ = 14%, and Z_0 = 50 Ω. Based on these requirements, the inverter constants J_nZ_0 (n = 1 ~ 4) of the bandpass filter can be calculated as $J_1Z_0 = J_4Z_0 = 0.4617$ and $J_2Z_0 = J_3Z_0 = 0.2021$. Also, the three parallel resonators in Fig. 7

(d) have the values of (L_n, C_n) = (2.068 nH, 2.041 pF), where n = 1, 2, and 3. Then, with a strip width w = 1.17 mm, the quality factor Q_A = 7.37 is obtained by using (12). This corresponds to a strip length l_1 = 10 mm from the Q_A–to-l_1 relationship shown in Fig. 5. To this point, all the dimensions of the inverted-L antenna are gotten, that is, l_1 = 10 mm, l_2 = 17.25 mm, and w = 1.17 mm. Hence, the radiation resistance R_A can be found as 28.6 Ω via Fig. 3(b).

Following, the inverter constant $J_3'Z_0$ of the third coupled line and thus the even- and odd-mode characteristic impedances Z_{0e3}' and Z_{0o3}' can be calculated by using (13) and (5), respectively, from which the line width and the gap between lines of the third coupled line are obtained. Note that these dimensions are dependent on the characteristic impedance Z_a used in the synthesis of the filtering antenna. Fig. 9 depicts their variations as functions of Z_a. It is seen that the larger is the impedance Z_a, the smaller the gap size is. When Z_a > 50 Ω, the gap would become smaller than 0.1 mm, which is difficult to realize. Thus, for easy fabrication, a characteristic impedance of Z_a = 30 Ω is selected here. This would correspond to an inverter constant $J_3'Z_0$ = 0.5515 and even- and odd-mode characteristic impedances (Z_{0e3}', Z_{0o3}') = (75.67 Ω, 42.58 Ω). Finally, the even- and odd-mode characteristic impedance of the first and second coupled line sections are calculated, using (14), as (Z_{0e1}, Z_{0o1}) = (83.74 Ω, 37.57 Ω) and (Z_{0e2}, Z_{0o2}) = (62.15 Ω, 41.94 Ω). The dimensions of each coupled line section for the proposed filtering antenna are shown in Table I. It should be noted that the gap size of the first coupled line section is extremely small and difficult to fabricate. To tackle this problem, the tapped structure with a quarter-wavelength impedance transformer [18] is utilized, as shown in Fig. 1(b).

From Fig. 3 (b), the antenna size of l_1 = 10 mm and w = 1.17 mm results in a parasitic capacitance of C_g = 0.365 pF in the equivalent circuit. The value of the capacitance C_g' shown in Block 2 of Fig. 7(c) is thus calculated as 0.04 pF from (10), which is indeed, as mentioned in the previous section, much smaller than the capacitance C_2' (=$C_2 - C_g'$ = 2.001 pF). Thus, $C_2 \approx C_2'$ is acceptable in the design.

The simulated return loss of the proposed filtering antenna (Fig. 1 (b)) in comparison with those of the traditional filter cascaded with antenna (Fig. 1 (a)) and the conventional third-order Chebyshev bandpass filter is shown in Fig. 10. Here, the conventional third-order Chebyshev bandpass filter has the same specifications as the filtering antenna (14% bandwidth and 0.1 dB equal- ripple response). For the traditional filter cascaded with antenna, the filter is a second-order Chebyshev bandpass filter with the same bandwidth and ripple level, and the antenna is an inverted-L antenna with (l_1, l_2) = (16.5 mm, 10 mm) for best impedance matching at the center frequency (2.45 GHz). It is observed that the bandwidth and skirt selectivity for the proposed filtering antenna agree very well with the conventional third-order Chebyshev bandpass filter, which demonstrates the design validity of the filtering antenna. On the other hand, putting an individually designed antenna after the (second-order) bandpass filter would, not only have no contribution to the order of the filter, but also deteriorate the original filter performance, especially resulting in bad skirt selectivity at the band edges.

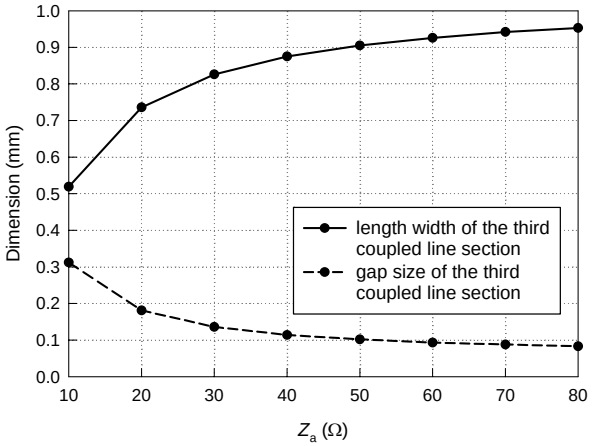

Fig. 9. Dimensions of the third coupled line section for different Z_a in the proposed filtering antenna.

TABLE I
DIMENSIONS OF EACH COUPLED LINE SECTION OF PROPOSED FILTERING ANTENNA

No. of coupled line section	Line width (mm)	Gap size (mm)	Length (mm)
1	0.746	0.054	18.8
2	1.063	0.254	18.6
3	0.831	0.138	18.6

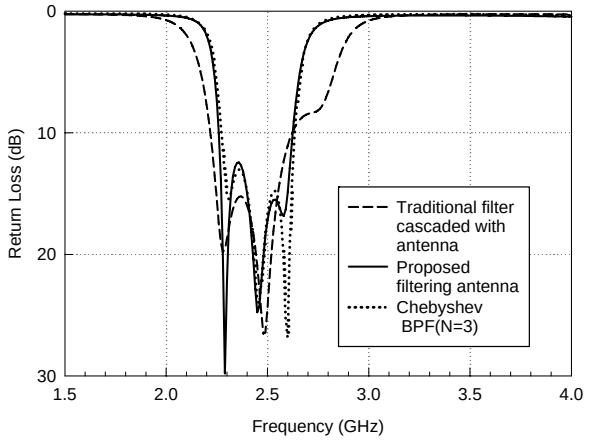

Fig. 10. Simulated return losses of the proposed filtering antenna, the conventional third-order Chebyshev bandpass filter (BPF), and the traditional filter cascaded with antenna.

Fig. 11 shows the simulated antenna gains versus frequency for the proposed filtering antenna and the traditional filter cascaded with antenna in the +*z* direction (Fig. 11 (a)) and the +*x* direction (Fig. 11 (b)). The simulated insertion loss of the conventional third-order Chebyshev bandpass filter is also shown for reference. Here, it is noticed that the antenna gain can be regarded as a normalized transmission power from the antenna's feed port to a remote pseudo port in the observation direction, and is thus analogous to the transmission power coefficient (or insertion loss) between the two ports of a filter. As compared to the traditional filter cascaded with antenna, the antenna gain of the proposed filtering antenna is flat in the passband and the bandwidth is very close to the insertion-loss bandwidth of the third-order Chebyshev bandpass filter. The maximum antenna gain is -1 dBi in the +*z* direction and -2.2 dBi in the +*x* direction. (Note that these values include the loss of the circuitry.) The proposed filtering antenna also provides better skirt selectivity with stopband suppression better than 22 dB.

It can be observed that the proposed filtering antenna have a radiation null at f = 2.15 GHz in the +*z* direction (Fig. 11 (a)) and at 3.25 GHz in the +*x* direction (Fig. 11 (b)), which makes the skirt selectivity even better than that of the conventional third-order Chebyshev bandpass filter. It is interesting to reason out how these nulls arise, since an inverted-L antenna alone should exhibit a monotonous gain dropping, but not a local gain

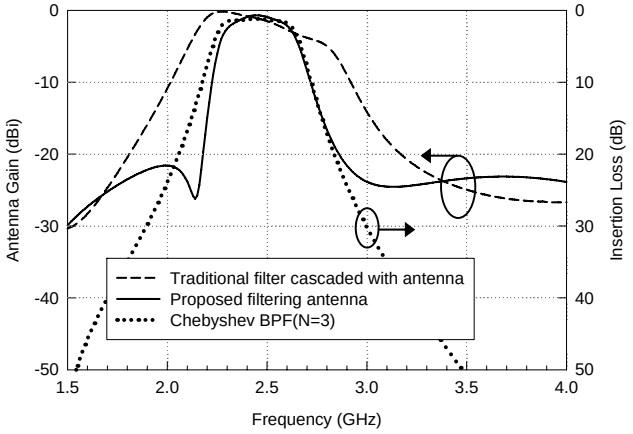

(a)

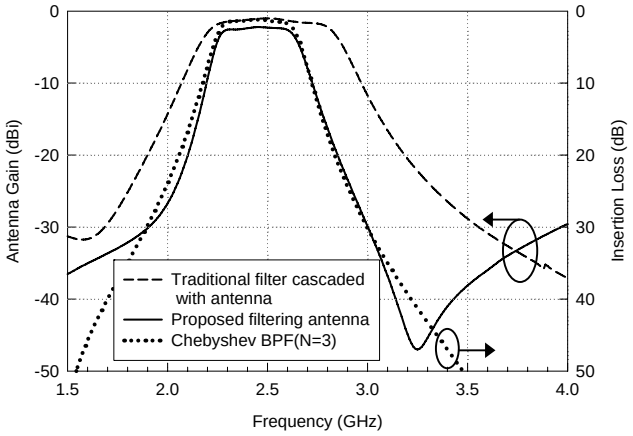

(b)

Fig. 11. Simulated antenna gains versus frequency of the proposed filtering antenna and the traditional filter cascaded with antenna in comparison with the simulated insertion loss of the conventional third-order Chebyshev bandpass filter (BPF). (a) In +*z* direction. (b) In +*x* direction.

minimum, when the operating frequency moves away from the antenna's resonant frequency. Also, since the frequency locations of these nulls depend on the observation angle, they are not caused by the circuit coupling between the first resonator and the third one (i.e., the inverted-L antenna) of the filter. It is finally found out that the last coupled line structure near the ground edge of the proposed filtering antenna (Fig. 1 (b)) induces a strong spurious ground edge current, which in turn produces extra radiation and cancels the radiation field from the antenna at some frequency in some direction. Fig. 12 shows the simulation radiation patterns in the *xz* plane at f = 2.15 GHz for the proposed filtering antenna (solid line) and a two-port

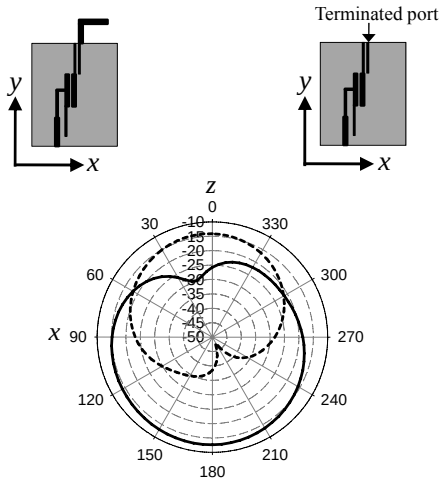

Fig. 12. Simulated total-field radiation patterns in the *xz* plane at $f = 2.15$ GHz for the proposed filtering antenna and a two-port circuit structure obtained from the filtering antenna with the inverted-L section replaced by a terminated port. [solid line: proposed filtering antenna; dashed line: two-port circuit structure.]

circuit structure obtained from the filtering antenna with the inverted-L section replaced by a terminated port (dashed line). It is seen that the two-port circuit does produce a spurious radiation toward the upper space (+*z* direction) with peak gain about -14 dBi. This spurious radiation field has about the same level as the omni-directional field pattern of an inverted-L antenna after the attenuation of the third-order bandpass filter at $f = 2.15$ GHz (see Fig. 11 (a)). Due to the field canceling, the total radiation pattern of the filtering antenna thus possesses a radiation null near the +*z* direction as shown in Fig. 12.

Fig. 13 compares the measured return losses of the proposed filtering antenna and the conventional third-order Chebyshev bandpass filter. The simulated return loss of the filtering antenna is also shown for comparison. Likely because of the deviations in dielectric constant and substrate thickness, the bandwidth of the measured return loss of the proposed filtering antenna is slightly narrower than the simulated one. However, it is in close agreement with the measured one of the conventional third-order Chebyshev bandpass filter. Both have the same passband poles' positions, the selectivity at the band edge, and the return-loss behavior at the stopband. This demonstrates that the proposed filtering antenna has good selectivity in accordance with the conventional bandpass filter.

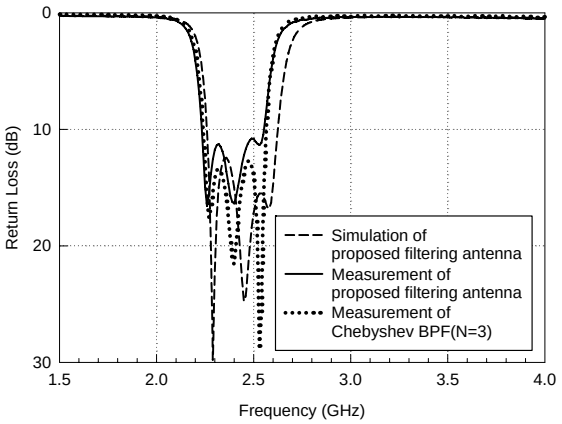

Fig. 13. Measured and simulated return losses of the proposed filtering antenna compared with the measured one of the conventional third-order Chebyshev bandpass filter (BPF).

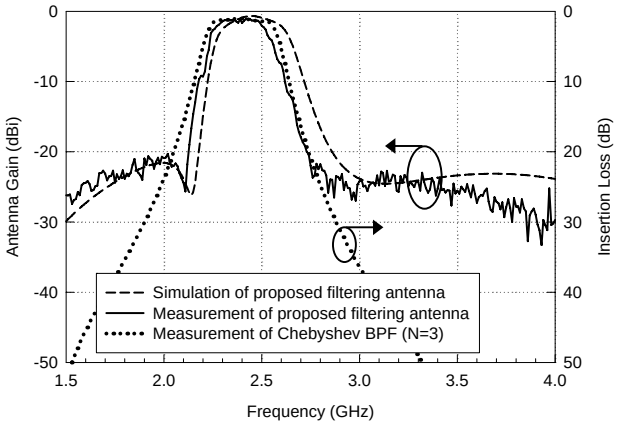

(a)

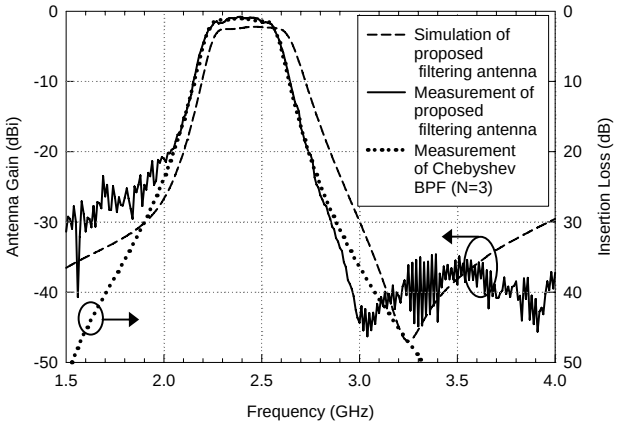

(b)

Fig. 14. Measured and simulated antenna gains versus frequency of the proposed filtering antenna in comparison with the measured insertion loss of the conventional third-order Chebyshev bandpass filter (BPF). (a) In the +*z* direction. (b) In the +*x* direction.

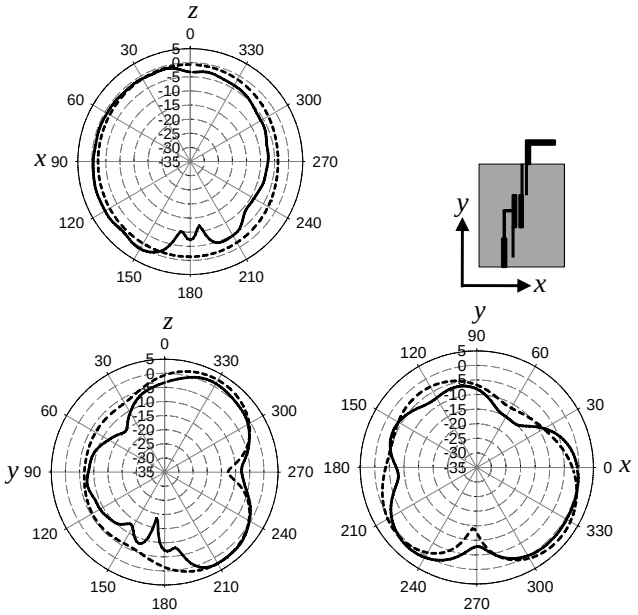

Fig. 15. Measured and simulated total-field radiation patterns in the *xz*, *yz*, and *xy* planes for the proposed filtering antenna. [solid line: measured results; dashed line: simulated results]. $f_0 = 2.45$ GHz.

TABLE II
SUMMARY OF ANTENNA PEAK GAINS OF THE FILTERING ANTENNA

Performances	Results	*xy*-plane	*yz*-plane	*xz*-plane
Peak Gain (dBi)	simulation	2.44	2.62	-0.67
	Measurement	1.13	2.34	0.65

The measured antenna gains versus frequency in the $+z$ direction and $+x$ direction for the proposed filtering antenna are depicted in Figs. 14 (a) and (b), respectively, which shows an antenna gain of -1.3 dBi in the $+z$ direction and -1.0 dBi in the $+x$ direction. It is obvious that the measured responses of the proposed filtering antenna have sharp skirt selectivity and similar to the measured results of conventional Chebyshev bandpass filter. The measured results match well to the simulated ones. Especially, the radiation nulls in low and high stopbands are clearly observed. The amplitude noise of the measured gain in the stopbands is due to the system noise of the antenna chamber.

The measured and simulated total-field radiation patterns at $f_0 = 2.45$ GHz in the three principal planes are also presented in Fig. 15. It is seen that the measured patterns are similar to the simulated ones, although a discrepancy occurs at $\theta = 180^\circ$ in the *yz* and *xz*-planes (that is, the $-z$ direction) due to the interference of the feeding coaxial cable in the measurement. The radiation pattern in the *xz*-plane is nearly omnidirectional with peak gain of 0.65 dBi. Table II summarizes the measured and simulated antenna peak gains in the three principal planes. Fig. 16 shows the photograph of the finished filtering antenna.

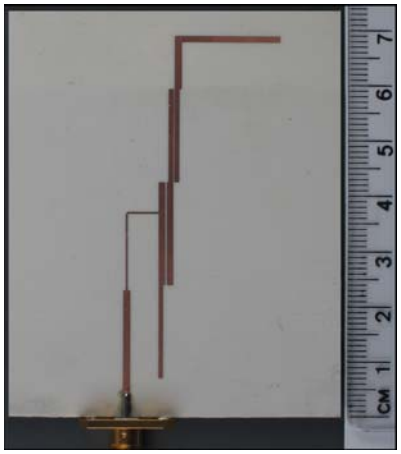

Fig. 16. Photograph of the finished filtering antenna.

V. CONCLUSION

In this proposal, a filtering antenna with new co-design approach has been proposed and implemented. The design is accomplished by first extracting the circuit model of the antenna, then casting it into the synthesis of a typical parallel coupled line filter. The antenna performs not only a radiator but also the last resonator of the filter. To increase the fabrication tolerance, a quarter-wave admittance inverter with characteristic impedance other than Z_0 is introduced in the filter synthesis. A design example which has the same specifications as the conventional third-order Chebyshev bandpass filter is demonstrated and presented. The measured results agree quite well with the simulated ones. The proposed filtering antenna provides good skirt selectivity as the conventional bandpass filter. It also possesses flat antenna gain in the passband and high suppression in the stopband. It may be of interest for future research that various types of filters can be utilized, which makes the circuit with better performance and compact size.

REFERENCES

[1] H. An, B. K. J. C. Nauwelaers, A. R. V. D. Capelle, "Broadband microstrip antenna design with the simplified real frequency technique," *IEEE Trans. Antennas Propag.*, vol. 42, pp. 129–135, Feb. 1994.

[2] B. Froppier, Y. Mahe, E. M. Cruz, and S. Toutain, "Integration of a filtering function in an electromagnetic horn," in *Proc. 33th Eur. Microw. Conf.*, 2003, pp. 939-942.

[3] F. Queudet, B. Froppier, Y. Mahe, and S. Toutain, "Study of a leaky waveguide for the design of filtering antennas," in *Proc. 33th Eur. Microw. Conf.*, 2003, pp. 943-946.

[4] G. Q. Luo, W. Hong, H. J. Tang, J. X. Chen, X. X. Yin, Z. Q. Kuai, and K. Wu, "Filtenna consisting of horn antenna and substrate integrated waveguide cavity FSS," *IEEE Trans. Antennas Propag.*, vol. 55, no. 1, pp. 92-98, Jan. 2007.

[5] F. Queudet, I. Pele, B. Froppier, Y. Mahe, and S. Toutain, "Integration of pass-band filters in patch antennas," in *Proc. 32th Eur. Microw. Conf.*, 2002, pp. 685-688.

[6] W.-G. Yeo, T.-Y. Seo, J. W. Lee, and C. S. Cho, "H-plane sectoral filtering horn antenna in PCB substrates using via fences at millmeter-wave," in *Proc. 37th Eur. Microw. Conf.*, 2007, pp. 818-821.

[7] J.-H. Lee, N. Kidera, S. Pinel, J. Laskar, and M. M. Tentzeris, "Fully integrated passive front-end solutions for a V-band LTCC wireless system," *Antennas Wireless Propag. Lett.*, vol. 6, pp. 285-288, 2007.

[8] N. Yang, C. Caloz, and K. Wu, " Co-designed CPS UWB filter-antenna system," in *Proc. IEEE AP-S Int. Symp.*, Jun. 2007, pp. 1433-1436.

[9] C.-H. Wu, C.-H. Wang, S.-Y. Chen, and C. H. Chen, "Balanced-to-unbalanced bandpass filters and the antenna applications," *IEEE Trans. Microw. Theory Tech.*, vol. 56, no. 11, pp. 2474-2482, Nov. 2008.

[10] M. Troubat, S. Bila, M. Thevenot, D. Baillargeat, T. Monediere, S. Verdeyme, and B. Jecko, "Mutual synthesis of combined microwave circuits applied to the design of a filter-antenna subsystem," *IEEE Trans. Microw. Theory Tech.*, vol. 55, no. 6, pp. 1182-1189, Jun. 2007.

[11] H. Blondeaux, D. Baillargeat, P. Leveque, S. Verdeyme, P. Vaudon, P. Guillon, A. Carlier, and Y. Cailloce, "Microwave device combining and radiating functions for telecommunication satellites," in *IEEE MTT-S Int. Microw. Symp. Dig.*, May 2001, pp. 137-140.

[12] T. L. Nadan, J. P. Coupez, S. Toutain, and C. Person, "Optimization and miniaturization of a filter/antenna multi-function module using a composite ceramic-foam substrate," in *IEEE MTT-S Int. Microw. Symp. Dig.*, Jun. 1999, pp. 219-222.

[13] S. Oda, S. Sakaguchi, H. Kanaya, R. K. Pokharel, and K. Yoshida, "Electrically small superconducting antennas with bandpass filters," *IEEE Trans. Appl. Supercond.*, vol. 17, no. 2, pp. 878-881, Jun. 2007.

[14] A. Abbaspour-Tamijani, J. Rizk, and G. Rebeiz, " Integration of filters and microstrip antennas," in *Proc. IEEE AP-S Int. Symp.*, Jun. 2002, pp. 874-877.

[15] W. L. Stutzman and G. A. Thiele, *Antenna Theory and Design*. New York: Wiley, 1998.

[16] High Frequency Structure Simulator (HFSS). Ansoft Corporation, Pittsburgh, PA, 2001.

[17] D. M. Pozar, *Microwave Engineering*, 3nd ed. New York: Wiley, 2005, ch. 8.

[18] M. Matsuo, H. Yabuki, and M. Makimoto, "The design of a half-wavelength resonator BPF with attenuation poles at desired frequencies," in *IEEE MTT-S Int. Microw. Symp. Dig.*, 2000, pp. 1181-1184.